Use of SIR-A and Landsat MSS Data in Mapping Shrub and Intershrub Vegetation at Koonamore, South Australia

Glen M. Green
McDonnell Center for the Space Sciences, Department of Earth and Planetary Sciences, Washington University, St. Louis, MO 63130

ABSTRACT: Shrublands cover much of the interior of the Australian continent and support a large grazing industry. Distinguishing the woody perennial vegetation from the smaller herbaceous vegetation and soil-encrusting lichen found between the shrubs is critical for range management but is difficult to do using Landsat data alone. In this study Shuttle Imaging Radar-A (SIR-A) and Landsat data acquired over Koonamore Station are examined together. Given the low topography and fine textured soils at Koonamore, radar return should be primarily determined by the percent area occupied by shrubs. During periods when most of the vegetation was non-vigorous and spectrally homogeneous, SIR-A data, as a surrogate measure of shrub cover, allowed the reflectance due to shrubs in Landsat data to be separated from the reflectance due to the intervening ground. This method allows estimation of the intershrub reflectance properties that are related to herbaceous vegetation, lichen, and bare soil exposures.

INTRODUCTION

SHRUBLANDS occupy about 46 percent of arid and semi-arid Australia and support approximately 20 million sheep, providing a major source of income for those regions (Moore, 1973). Distinguishing the woody perennial vegetation (shrub component) from the herbaceous plants and lichen that grow between the shrubs (intershrub component) is desirable because grazing is affected differently by these contrasting vegetation components. Herbaceous plants are generally the preferred fodder of sheep except in times of drought when sheep browse almost exclusively on those palatable shrubs within their reach (Osborn *et al.*, 1932, 1931). Moreover, the effects of grazing on herbaceous plants, shrubs, and lichen vary considerably (Rogers and Lange, 1971; Crisp, 1978). Therefore, in order to provide a reasonable inventory of shrublands, the monitoring of *both* vegetation components is necessary. Extensive, detailed ground surveys that are necessary in formulating a sound range management policy are difficult to justify because of the low productivity per hectare of land. Data from remote sensing, with a broad field of view, contains information on vegetation cover and can provide an effective alternative method of range inventory.

The shrub and intershrub components cannot be easily distinguished using Landsat Multispectral Scanner data (MSS) alone because the reflectance spectra for shrubs and grasses may be similar when both are in either vigorous or non-vigorous states (Graetz and Gentle, 1982; Graetz *et al.*, 1982). Furthermore, variation in the amount of either shrub cover, or grass and lichen cover, prevents the straightforward and independent mapping of shrubs or intervening materials (Tueller *et al.*, 1978; Kornblau *et al.*, 1983). Most techniques used to separate woody perennial vegetation from the intershrub vegetation component have employed the contrasting phenological response of shrub and herbaceous plants to seasonal precipitation (Lane, 1982; Musick, 1984). The differing response is mainly a function of the depth and density of plant roots (Walter, 1979). MSS images are examined during times when the vegetation of one component is vigorous and the other is in a non-vigorous state, thereby maximizing the spectral reflectance contrast between them.

An approach that uses phenology is limited by the following constraints: (1) rainfall in semi-arid regions can be quite variable both seasonally and from year to year, so the detailed climatic history of the region under investigation must be known (Hall *et al.*, 1964), (2) rain, generally supplied by thunderstorms in these environments, may be very local in distribution (Carrodus *et al.*, 1965), (3) the phenological responses of species to rainfall events differs and must be known (Noble, 1977), and (4) microtopographic and edaphic changes can greatly affect the responses of plants to given rainfall events (Crisp, 1975; Walter, 1979). These complications could

PHOTOGRAMMETRIC ENGINEERING AND REMOTE SENSING,
Vol. 52, No. 5, May 1986, pp. 659–670.

0099-1112/86/5205-659$02.25/0

be avoided if the first-order morphological differences between the shrub and intershrub vegetation components could be determined and used to separate the components.

In this study Shuttle Imaging Rada-A (SIR-A) data (Elachi *et al.*, 1982) are examined together with Landsat MSS data to demonstrate a morphological approach to the remote sensing of an Australian semi-arid shrubland. Radar backscatter at the SIR-A wavelength (23.5 cm) and incidence angle (50 degrees) is controlled in the test area primarily by surface roughness. The magnitude of roughness is a function of the volume geometry of the vegetation relative to the incident wavelength and, therefore, should be sensitive to the large morphological differences between woody perennial vegetation and intershrub vegetation, with the former producing much higher returns. SIR-A data, as a surrogate measure of shrub cover, thus permits the reflectance due to woody perennial vegetation in Landsat data to be separated from the reflectance due to the intervening ground. This method allows estimation of the intershrub reflectance properties that are related to herbaceous vegetation, lichen, and bare soil exposures, and indicates that the distributions of shrub and intershrub vegetation can be effectively mapped.

STUDY SITE

The study area covered by the SIR-A and Landsat MSS data is located within Koonamore Station, a sheep grazing ranch in South Australia (Figure 1). This site was chosen because it contains representative vegetation found throughout semi-arid Australia (Moore, 1973), and because the Station has been the site of a number of case studies of land cover (e.g., Hall *et al.*, 1964; Crisp, 1975). The vegetation of Koonamore Station can be divided into two contrasting components on the basis of their life-form: (1) woody perennial vegetation, consisting of (a) *Eucalyptus* sp. and other trees, (b) tall arborescent shrubs like *Acacia* sp., and (c) the low intricately branched Chenopodiaceous shrubs of genera like *Atriplex* and *Maireana*; and (2) vegetation found between these woody plants: (a) small herbaceous grasses and forbs, and (b) soil-encrusting lichens (Carrodus *et al.*, 1965; Rogers, 1974). The appearance of these plants in cross section is shown in Figure 2. For reference, Figure 3 is a vegetation map from Carrodus *et al.* (1965) of a portion of Koonamore Station, showing the distribution of the dominant vegetation associations, together with dry salt-lakes and gypsum covered soils.

Koonamore Station has a relatively well-known grazing history that began in the late 1800s, and contains the T.G.B. Osborn Vegetation Reserve (OVR), an area that was fenced from South Lake Paddock (SLP), located to the northwest, in 1925. From 1925 to the present, sheep have been excluded from the OVR, and rabbits have been kept at very low numbers since the mid 1970s. The regeneration of the natural vegetation in the Reserve, and the condition of the vegetation still being grazed outside the OVR, have been extensively studied in the field since 1925 (Silander, 1983). Thus, this region provides good control with regard to grazing history and regeneration.

ANALYSIS OF LANDSAT MSS DATA

Koonamore Station was imaged by the Landsat 3 Multispectral Scanner (MSS) on 16 October 1981. The MSS has four bands whose approximate bandpass intervals as well as other sensor characteristics are shown in Table 1. Data for each of the four bands were first calibrated for sensor gain and offset and for solar incidence angle to yield bi-directional normal reflectance values, assuming a Lambertian reflecting surface. The methods used are outlined in Robinove (1982). Corrections were then made for atmospheric scattering and absorption effects, assuming an optically thin atmosphere appropriate for desert conditions (Otterman *et al.*, 1981; Richardson, 1981). The four band corrected data, which have values proportional to the ground bi-directional reflectance, were then geometrically registered to the vegetation map in Figure 3 using nearest neighbor resampling.

For comparison, Graetz and Gentle (1982) obtained a large number of bi-directional field spectral reflectance values, corresponding to the MSS wavebands, for soil and vegetation in various states of vigor in Australia. Measurements were taken within

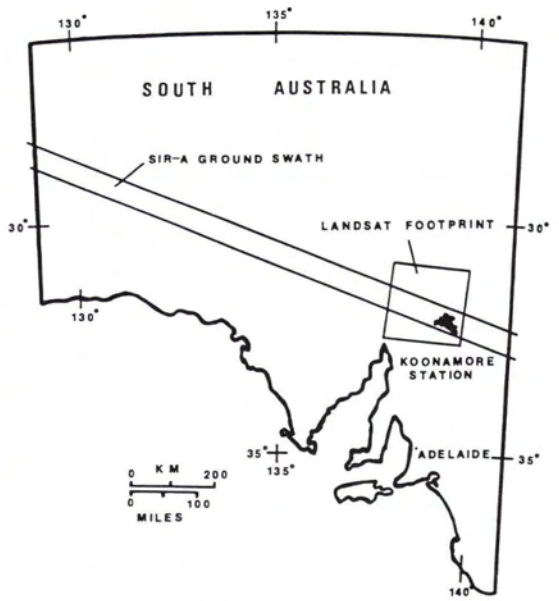

FIG. 1. Location map, showing Koonamore Station in South Australia, along with the locations of the SIR-A swath (orbit 31) and Landsat 3 frame used in this work.

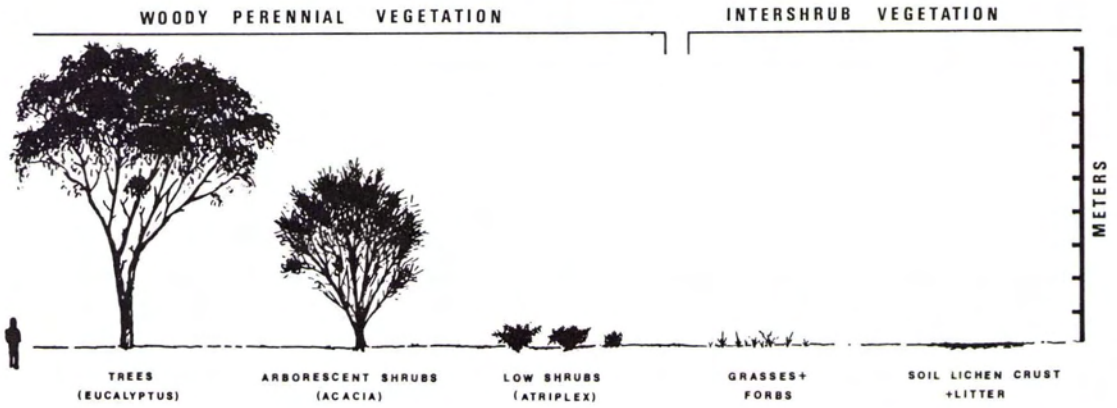

FIG. 2. Sketch illustrating the morphology and relative sizes of woody perennial and intershrub vegetation of semi-arid Australian shrubland at Koonamore.

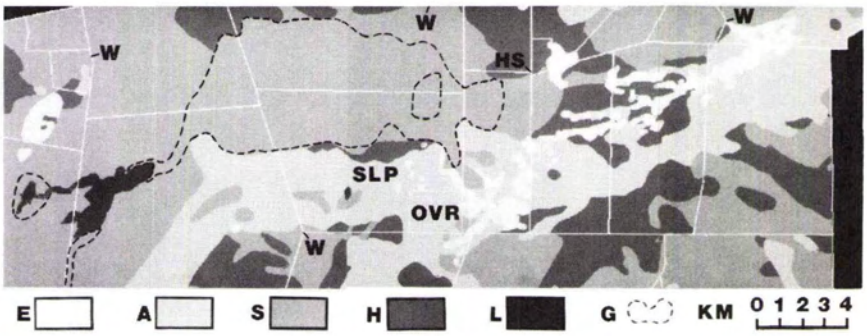

FIG. 3. Vegetation map of a portion of Koonamore station, from Carrodus *et al.* (1965). HS is the Head Station, OVR = T.G.B. Osborn Vegetation Reserve, SLP = South Lake Paddock, W = sheep watering wells. Shown is the distribution of various vegetation associations named for the dominant species; E = discontinuous stratum of *Eucalyptus oleosa* with an understory of low shrubs and herbaceous ephemeral plants; A = discontinuous stratum of *Acacia* sp and *Eremophlia* sp with an understory of low shrubs and herbaceous ephemerals; S = low shrubs of *Atriplex*, *Marieana*, and *Nitraria* sp with herbaceous ephemerals between; H = woody vegetation largely absent and covered by herbaceous forbs or grasses like *Stipa nitida* and *Bassia* sp; L = dry salt-lake deposits; G = area of gypsum covered soils. Bare ground in all associations may be covered locally by soil crusting lichens. White lines denote fence boundaries. North is to the top of the image. Black regions at the eastern edge and northwest corner are unmapped.

50 kilometres of Broken Hill, about 200 kilometres to the east of the study site, in an *Atriplex* shrubland similar to that found at Koonamore. He found that, except for vigorous vegetation, all cover types exhibit spectral reflectance curves of similar shape, but differ by a factor of four in magnitude. Most soils were shown to have high reflectance values, and eroded soils were the brightest materials in the area. Eroded soils have generally been deflated of fine clays by winds, leaving a quartz rich residuum of high spectral reflectance. All non-vigorous vegetation (perennial shrubs and grasses), together with lichen-encrusted soils, exhibit relatively low reflectance values.

These data suggest that, at MSS wavelengths, much of the information concerning non-vigorous shrubland vegetation cover can be expressed as a variation in brightness (Graetz *et al.*, 1982). Summed MSS bi-directional reflectance or albedo, as defined by Robinove *et al.* (1981), has been used extensively as an indicator of vegetation cover in other semi-arid terrain (Courel and Habif, 1983; Frank, 1984). The reflectance values of Graetz and Gentle (1982) were thus summed to albedo terms and are shown in Table 2, together with an albedo value for gypsum encrusted ground from Munday (1982). These values provide a basis for interpretation of an albedo image (Figure 4) produced by summing the four band Landsat MSS bi-directional ground reflectance data for the study site.

Brightness indices such as albedo do not effectively distinguish actively growing vigorous vege-

TABLE 1. SENSOR CHARACTERISTICS

Landsat-3 MSS		SIR-A	
Date	16 Oct 1981	Date	13 Nov 1981
Scene ID	E-31321-23520	Orbit No.	31
Band 4 (micrometres)	0.5-0.6	Frequency (GHz)	1.278
Band 5	0.6-0.7	Wavelength (cm)	23.5
Band 6	0.7-0.8	Look Angle (deg)	47 ± 3
Band 7	0.8-1.1	Incidence Angle (deg)	50 ± 3
Solar Incidence Angle	43 (deg)	Polarization	HH
Footprint Size (km)	185	Swath Width (km)	50
Picture Element Width	79 (m)	Picture Element Width	40 (m)

TABLE 2. MEAN ALBEDO VALUES (PERCENT) AND STANDARD ERRORS AS DEFINED BY ROBINOVE ET AL. (1981) FROM FIELD REFLECTIVE DATA OF GRAETZ AND GENTLE (1982) AND MUNDAY (1982)*

Bare Soil	Gypsum Covered (*)	41
	Eroded	40 ± 4
	Undisturbed	29 ± 4
	Calcareous	26 ± 4
	Lichen Crusted	16 ± 3
Shrub (*Atriplex*)	Vigorous	28 ± 4
	Non-Vigorous	13 ± 1
Grass	Vigorous	28 ± 9
	Non-Vigorous	11 ± 3
Herbaceous Ephemerals	Vigorous	26 ± 4
Litter	Shrub + Grass	9 ± 1
Shadow		1 ± 1

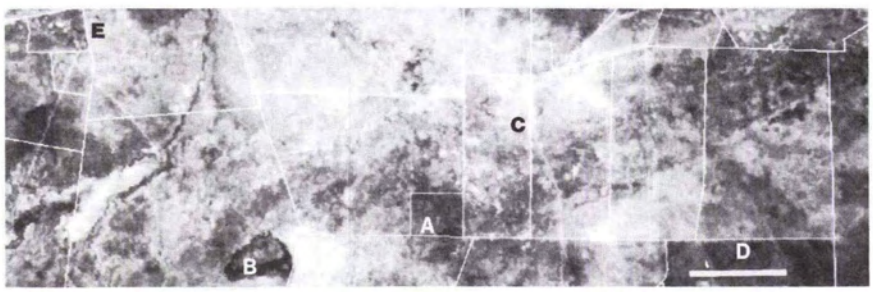

FIG. 4. Landsat MSS albedo image for Koonamore Station, generated by methods discussed in the text. Bright tones denote areas of high albedo while dark tones denote areas of low albedo. Albedos range from 0.1 to 0.35. White lines denote fence boundaries. Area directly to the right of A = region of dense *Casuarina cristata* trees; B = shrubless ground covered by herbaceous plants; C, D, and E = regions of contrasting albedo across fence lines produced by differing degrees of sheep grazing and trampling. Scale bar at lower right is 4 kilometres long.

tation from other materials and, as such, would be appropriate only for vegetation in a non-vigorous state. Examination of the MSS data processed to show greenness indices (not shown), as described in Graetz *et al.* (1982) and Musick (1984), reveals that vigorous vegetation was minimal at Koonamore when the Landsat scene was acquired. The vigorous component was found to be restricted primarily within the *Eucalyptus* and to a lesser extent to the *Acacia* vegetation associations in Figure 3. Daily weather observations taken at Koonamore Head Station (available through the Australian Bureau of Meteorology) show that there had not been an "effective" rainfall, as defined by Osborn *et al.* (1935), for approximately 3 months prior to the Landsat overpass. Given the climatic conditions, a majority of the vegetation is expected to be in a non-vigorous state.

Albedo histograms extracted from the albedo image for each of the Koonamore vegetation association units of Carrodus *et al.* (1965) are shown in Figure 5a. These plots reveal a decrease in albedo

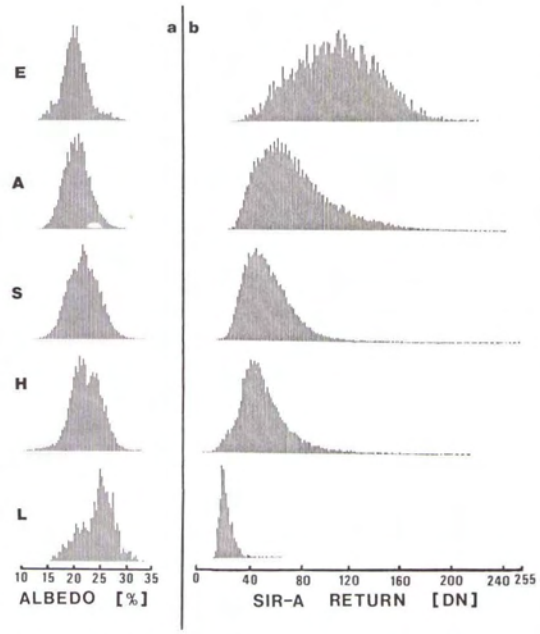

FIG. 5. (a) Albedo versus frequency plots (histograms) of various vegetation associations from Figure 3. Albedo generally decreases with increasing woody perennial vegetation. SIR-A radar return histograms of various vegetation associations. SIR-A return generally increases with increasing perennial vegetation.

from dry salt-lake (L) through the shrubless ground (H) and low shrub units (S) to the vegetation units of the *Acacia* (A) and *Eucalyptus* (E) associations. This transition probably reflects increasing woody perennial vegetation cover, similar to that observed by Howard (1977). The dry salt lakes (average albedo 0.25) are bare of all vegetation. In those regions where low shrubs are dominant (average albedo 0.22), the shrubs are usually separated by at least one plant diameter while, within the *Acacia* and *Eucalyptus* vegetation associations (average albedos of 0.21 and 0.20, respectively), low shrubs often form an understory between the trees and arborescent shrubs (Russell Sinclair, University of Adelaide, Dept. of Botany, Koonamore Officer, unpublished data, 1985). An area with one of the lowest albedos (0.15), found in the *Acacia* association unit in the southeast corner of the OVR (Figure 4, A), also has one of the densest tree canopies (*Casuarina cristata*) within the study site (Sinclair, unpublished data, 1985). Thus, the observed albedo within an MSS picture element can be controlled by the percent cover of woody perennial vegetation.

Because shrubland woody perennial cover is generally less than 30 percent (Graetz and Gentle, 1982), the albedo of an area should also be controlled in large part by the intershrub material. A change in the cover of soil lichen crust or herbaceous plants, a quartz sand residuum left by erosion of bare soil, or the presence of a salt crust on the soil surface may also contribute to a change in albedo. One instance where herbaceous plant cover produces an albedo similar to that produced by shrub cover is shown in Figure (4B). Within the shrubless unit of Figure 3, cover of the herbaceous plant *Erodiophyllum* leads to an albedo of 0.13, lower than any in the *Acacia* or *Eucalyptus* association units (Carrodus *et al.*, 1965)(see Figure 5).

The relationship between albedo, shrub cover, and intershrub ground material for non-vigorous vegetation is shown diagrammatically in Figure 6. The figure employs the reflectance values of Graetz and Gentle (1982) and Munday (1982). The effects of shrub shadowing are not included because they are a function of solar incidence angle and, thus, vary with season and time of day. At the time when the Landsat image was acquired (near summer), shadowing effects are expected to lower the mixing line between eroded soil and 100 percent shrub cover by <10 percent. The effect on darker ground cover would be less. The suggested linear relationships are consistent with a model of the reflectance of shrublands where the shrubs are assumed to contribute to the signal in direct proportion to the fractional area covered by these plants. The stippled portion of the plot shows the possible range of albedos expected at Koonamore. The range of albedo values should decrease and the albedos should converge to that of non-vigorous shrubs at high shrub cover percentage. The similar albedos of 100 percent bare undisturbed soil (0 percent shrub cover) and eroded soil with 40 percent shrub cover demon-

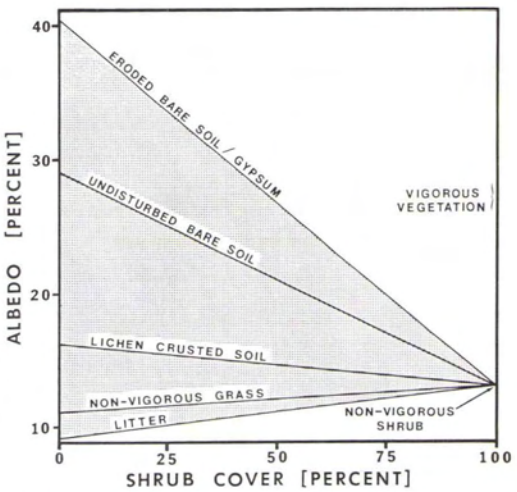

FIG. 6. Diagrammetic relationship between albedo, woody perennial vegetation cover, and intershrub ground condition, assuming vegetation is non-vigorous and that there is no shadowing. Albedo values are calculated from Graetz and Gentle (1982) and Munday (1982). Stippled pattern denotes field of probable values for a semi-arid shrubland after an extended dry period. Albedo values converge to that of non-vigorous shrubs with higher shrub cover.

strate the ambiguity in making estimations of cover from MSS albedo data alone. If percent shrub cover were known, however, albedo would give a clear indication of the intershrub ground material.

The MSS albedo image shows areas of contrasting albedo across many fence boundaries (Figure 4 (C, D, and E)). The contrast probably reflects changes in either the woody perennial vegetation component or the intershrub vegetation component due to the effects of sheep. Sheep graze preferentially on grasses and forbs, and, in addition, soil lichens are rapidly destroyed by the trampling of sheep, especially near wells (Rogers and Lange, 1971). Soil is subject to erosion where the lichen crust has been destroyed. Many of these "scalded" areas will not support vegetation, even after rainfall (Wood, 1936). A reduction of the intershrub vegetation cover by grazing and trampling would be limited in location by fencing and, therefore, may produce the across-fence albedo contrast observed.

ANALYSIS OF SIR-A DATA

Koonamore Station was imaged by SIR-A on orbit 31 on 13 November 1981 (Table 1). The original SIR-A film product was digitized to 255 grey levels using a microdensitometer with a 60-micrometre spacing. This spacing resulted in a picture element width of 25 metres, roughly 2 times the spatial frequency of the original image (40 metres along and across track), thereby preserving the original resolution in the digitization process. A 3 by 3 median filter was applied to the SIR-A image to reduce the effects of speckle (Blom and Daily, 1982). Both *Acacia* and *Atriplex* communities in Australia have been shown to display a largely random distribution (Slatyer, 1973) at the resulting effective sampling widths for both the SIR-A and Landsat data. Topography in the study area varies by only several metres (Carrodus *et al.*, 1965), so that radar relief displacement and return due to slopes should be negligible. The processed SIR-A image was geometrically registered to the vegetation map of Koonamore (Figure 3) by nearest neighbor resampling, using ground control points taken mostly at fence intersections.

Radar backscatter from vegetation is governed predominantly by two target parameters: (1) roughness, a function of the volume geometry of the vegetation, and (2) the dielectric properties of the vegetation, mainly a function of plant water content (Ulaby, 1981). Morain and Simonett (1966) have examined radar images of arid shrublands in the Escalante Valley, Utah. They found that radar returns for shrublands are primarily influenced by the percentage of ground covered by shrub vegetation. Where variations in height of the vegetation were accompanied by changes in life-form, for example from shrub to grass, there were significant variations in radar return. Similar effects of shrub cover on radar return were noted by Morain and Campbell (1974) for K- and X-band radar, and by Blom and Elachi (1981) and Honey and Tapley (1982) for L-band systems. Morain and Campbell (1974) suspect that radar return from shrubs in a desert terrain would not be influenced greatly by low plant moisture contents, and, thus, radar return variation should be limited to roughness differences.

The soil surface at Koonamore is dominantly sand and fine silt with local small calcareous pebbles (Osborn *et al*,. 1932; Roger, 1974). These soil irregularities, together with those produced by the development of a lichen crust, scalds, or sparse non-vigorous herbaceous plants, result in roughness heights smaller than the 5-cm limit for the Rayleigh criterion for specular reflection (Roger, 1974; Osborn *et al.*, 1931; Hall *et al.*, 1964, see photos). The Rayleigh criterion for a surface that specularly scatters incident radar is given by:

$$h < \lambda/8\cos\theta \qquad (1)$$

where h is the height of irregularities in the surface, λ is the radar wavelength, and θ is the radar incidence angle. For SIR-A, surfaces with irregularities less than 5 cm would be considered radar smooth and would be specular scatterers. The low moisture content of the soils, implied by the dry climatic history at Koonamore, should also minimize the ground contribution to radar backscatter. Thus, the percent woody perennial vegetation cover should control radar backscatter while variation in the intershrub ground material (which has a substantial influence on albedo) probably has little effect on SIR-A backscatter.

Figure 7 shows the SIR-A image of the study site overlaid with fence boundaries. Histograms of radar return for each of the vegetation association units of Figure 3 are shown in Figure 5b. These plots reveal an increase in SIR-A backscatter from the very low relative radar returns of the dry salt-lake unit (L)(Figure 7(A)), through the shrubless (H) and low shrub (S) vegetation associations, to higher returns for the *Acacia* (A) and *Eucalyptus* (E) association units. The trend probably reflects increasing radar return with increasing cover of woody perennial vegetation, in the same manner that albedo is observed to decrease with increasing woody cover. Some of the highest returns are located within the same dense tree cover in the OVR (Figure 7(B)) that exhibited low MSS albedo in Figure 4 (A).

Note that, while the relative decrease in albedo between the *Acacia* and *Eucalyptus* associations is slight and similar to that change between other adjacent units in Figure 5a, the SIR-A backscatter for the *Eucalyptus* unit is significantly greater than that of the *Acacia* units compared to those differences between the radar return of other adjacent units in Figure 5b. The high radar return for the *Eucalyptus* association can be used to map its distribution. A density slice of the SIR-A image correctly classified 75 percent of those areas mapped by Carrodus *et al.* (1965) as *Eucalyptus* while misclassifying 28 percent of the *Acacia* association and less than 10 percent of

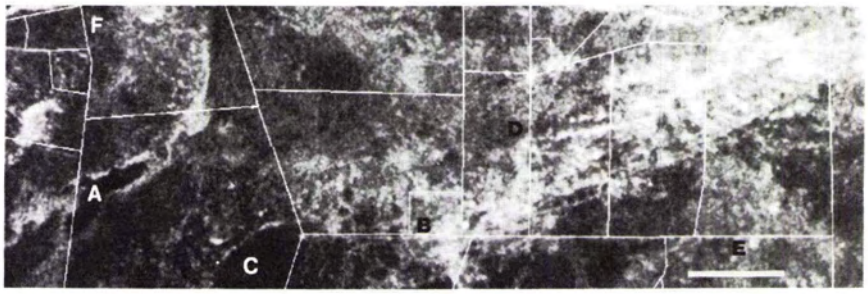

FIG. 7. SIR-A radar image for Koonamore Station, overlain with fence boundaries. Bright tones denote areas of high radar return while dark tones denote areas of low radar return. Radar return in this area is controlled predominantly by woody perennial vegetation cover. A = dry salt lake bare of all vegetation; immediately east of B = area of dense tree canopy; C = shrubless area covered by herbaceous plants; north of D = region covered almost exclusively by large clumps of unpalatable shrub; regions D, E, and F exhibit marked albedo differences across fences but show little contrast in radar return. Scale bar at lower right is 4 kilometres long.

the other associations as *Eucalyptus*. The anomalously high radar backscatter from the *Eucalyptus* association is probably related to the large volume per area of cover of the *Eucalyptus* tree relative to that of the other woody species at Koonamore (Figure 2).

COMPARISONS OF LANDSAT AND SIR-A DATA

The trends discussed above and examination of the albedo and radar images suggest an inverse relationship between Landsat-derived albedos and SIR-A returns. To further explore this relationship, logarithms of the SIR-A brightness values were taken to convert the SIR-A histogram to a Gaussian distribution. The conversion to a Gaussian distribution facilitates the application of linear methods, such as computing correlation coefficients, to the analysis of SIR-A and Landsat data. Because the SIR-A data will be calibrated in a relative way based on ground truth, the transformation does not alias the results. A linear correlation coefficent of -0.337 between log SIR-A and Landsat albedo data hints that as radar return increases albedo decreases, although the low correlation demonstrates that there is also independent information in the SIR-A data.

An example of these other controls on albedo, beyond the inverse correlation with SIR-A return, is shown at (C) in the SIR-A image (Figure 7). In the albedo image (Figure 4) this area had a very low albedo (0.13), while the SIR-A image also shows a low corresponding radar return, contrary to that predicted given a simple inverse relationship. The small non-vigorous herbaceous plants at this location, while producing a very low albedo, probably do not contribute substantially to the radar backscatter because of their small size, at SIR-A wavelengths (23.5 cm), thus providing low returns in both MSS and SIR-A data.

As another example of variations beyond a linear relationship, the SIR-A image, in contrast to the MSS albedo image, shows few differences in radar return across fence boundaries (Figure 7 (D,E, and F). To illustrate, a region near the Head Station was examined in detail. Figure 4(C) shows an area of high albedo to the southwest of the Head Station; the albedo decreases gradually as one moves radially to the southwest. The albedo abruptly decreases across the fence to the east. The SIR-A image shows no corresponding changes in radar return across the fence (Figure 7 (D)). This observation suggests that the increased MSS albedo near the Head Station is caused by a decrease in the intershrub vegetation and not by a decrease in shrub cover. Ground observations show that the area to the southwest of the Head Station is covered almost exclusively by large clumps of the shrub *Nitraria schoberi*, which is relatively unpalatable and resists grazing (Sinclair, unpublished data, 1985). The soil between the shrubs is very disturbed and the lichen crust has been destroyed due to the trampling of sheep brought to the Head Station to be shorn. Generally, large woody perennial vegetation is largely undisturbed by sheep because it grows beyond their reach. Thus, albedo changes across fences that are not associated with a change in radar returns are probably due to changes in the intershrub soil or vegetation cover.

Local phenomena that impact the general inverse relationship between albedo and SIR-A return are now considered. Ulaby (1981) and Henninger and Carney (1983) have demonstrated the increased accuracy of classification of agricultural and forested lands by using MSS and radar data, as opposed to using MSS data alone. The methodology of comparing optical and radar data has received some attention (Daily *et al.*, 1979). However, digital integration of SIR-A data with MSS data is hampered by lack of calibration data for the SIR-A sensor (Elachi *et al.*, 1982). Digital analysis is further limited by a lack of calibrated radar backscatter data versus shrub cover

for different semi-arid woody species and states of plant vigor. While the exact relationship between radar backscatter and semi-arid woody perennial vegetation cover at Koonamore is not known, the relationship is approximated here by setting the logarithms of the SIR-A radar return of the dry salt-lake to 0 percent woody vegetation cover and that of the southeast corner of the OVR that is covered by dense woods to 100 percent. The remaining log SIR-A values were scaled linearly between these two extremes. Because only the spatial distribution of the relative value of these data will be examined, neither the assumption of linearity nor the lack of SIR-A calibration should greatly affect the observed trends.

Scatter plots of the logarithm of SIR-A radar return data versus MSS albedo for the various vegetation associations of Figure 3 are shown in Figure 8. Overlaid on these plots are the boundaries of the expected values of albedo versus percent shrub cover from Figure 6 and contour lines at 20 percent intervals. Generally, most of the data in Figure 8 fall within the boundaries of the materials expected at Koonamore, given its recent dry climatic history, with the exception of the *Eucalyptus* association. Data in the dry salt lake region (L) clusters in the middle left of the diagram, consistent with relatively bright bare ground. Within the low shrub association (S), and within the association where herbaceous vegetation dominates (H), at higher SIR-A values the range of albedo values decreases and the albedos approach the reflectance of non-vigorous shrubs as measured by Graetz and Gentle (1982). This would be expected given a decreasing contribution of the intershrub ground component to the overall albedo at high percent shrub cover. Data within the mapped *Eucalyptus*, and to a lesser extent the *Acacia* associations, plot above and to the right of the expected field. This probably reflects high volume scattering of the *Eucalyptus* trees, relative to their cover, as well as a contribution from vigorous vegetation observed within these associations in MSS 'greenness" images. This latter affect would lead to an increase in albedo above expected values with increasing woody vegetation cover.

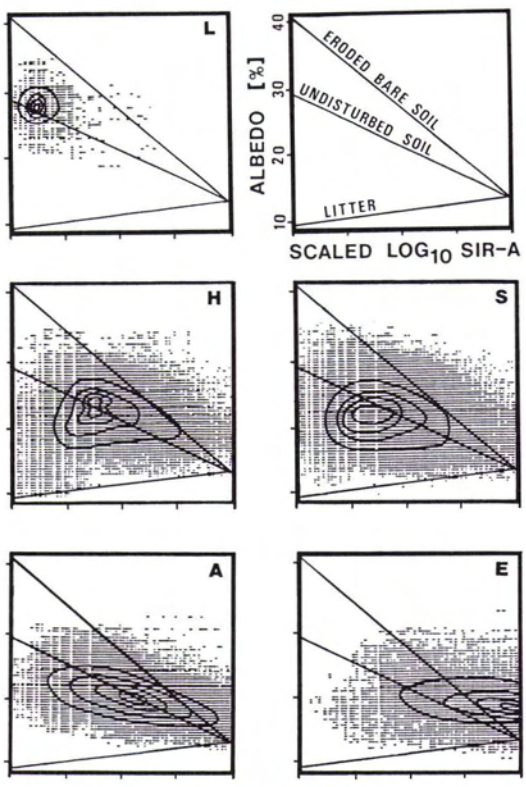

FIG. 8. Scatter plots of the logarithms of SIR-A return versus MSS albedo for the vegetation associations from Figure 3. Contour lines are drawn at 20 percent intervals. Overlain on the plots is the boundry of the expected values for materials at Koonamore from Figure 6. Variations in albedo generally decrease with increasing SIR-A return.

INTERSHRUB GROUND ALBEDO

The intershrub ground albedo is now calculated using the SIR-A data as a surrogate measure of the woody perennial vegetation cover. The albedo of a given MSS picture element (pixel) is a summation of all the albedos of the materials within the pixel multiplied by the fraction of the pixel they cover. The effect of shadows produced by predominantly vertical plants has been modeled by Otterman and Robinove (1983). Shadowing of the intershrub ground by low shrubs has been modeled by Graetz and Gentle (1982) and is a function of the solar incidence angle, percent shrub cover, and plant shape. Overall albedo is a function of the albedos of the shrub and intershrub components as well as shadowing. An assumed relationship describing the albedo is given below and diagrammed in Figure 9:

$$A_g = \frac{A_t - SA_w - B(1-S)A_s}{(1-S)-B(1-S)} \qquad (2)$$

where A_g is the subpixel albedo of the intershrub ground component, A_t is the average overall pixel albedo as measured by the Landsat MSS, A_w is the albedo of the perennial woody vegetation component, A_s is the albedo of shrub shadows, S is the fractional cover of the pixel by shrubs as determined by the SIR-A data, 1-S is the fractional cover of the pixel by intershrub ground and, B is the fraction of intershrub ground in shadow (a function of S and i, the solar incidence angle).

The intershrub ground albedo was calculated using Equation 2 and the SIR-A data as a surrogate measure of shrub cover, calibrated as described previously. The albedo values of shrubs (assumed to be non-vigorous) and shadow are from Graetz and Gentle (1982) (Table 2). Shadow percent was computed from the curves of Graetz and Gentle (1982)

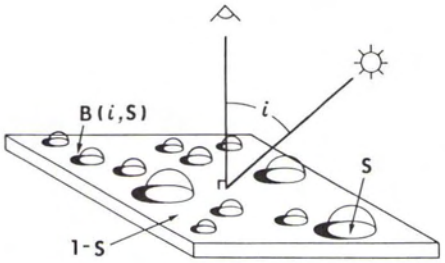

FIG. 9. Schematic view of an idealized shrubland pixel, where S is the fraction of pixel covered by shrubs, $1-S$ is the fraction of the pixel covered by intershrub ground, B is that fraction of the intershrub ground in shadow at a given S and i, the solar incidence angle (as modeled by Graetz *et al.* (1982a)).

using the curve for $i=40$ degrees (scene $i=43$ degrees). The derived intershrub ground albedos are shown in Figure 10. As percent shrub cover increases, the influence of shrub albedo also increases. Conversely, the influence of the intershrub ground albedo on the overall albedo diminishes such that, at 100 percent shrub cover, the ground albedo exercises no control on the overall albedo. Therefore, only regions with SIR-A returns calibrated to less than 60 percent woody perennial vegetation cover are considered to exclude those areas where accurate intershrub ground albedo determinations are less likely. A majority of the *Eucalyptus* association unit and that fraction of the *Acacia* association that exhibit the highest SIR-A returns are removed from further analysis in this manner. These excluded regions account for 15 percent of the study area and include the southeast portion of the OVR.

The method used for determining intershrub ground albedo, outlined above, is valid only for those shrubland communities in which woody plants have similar non-vigorous albedo, shadowing, and volume scattering as those assumed; the values for these parameters correspond to those for low shrubs. As such, the method may be inappropriate for *Eucalyptus* communities due to the large morphological differences noted earlier.

Figure 10a shows all regions that have computed intershrub albedos greater than 0.35 (an albedo of a shrubless model pixel with 50 percent eroded soil and 50 percent undisturbed soil) as black areas.

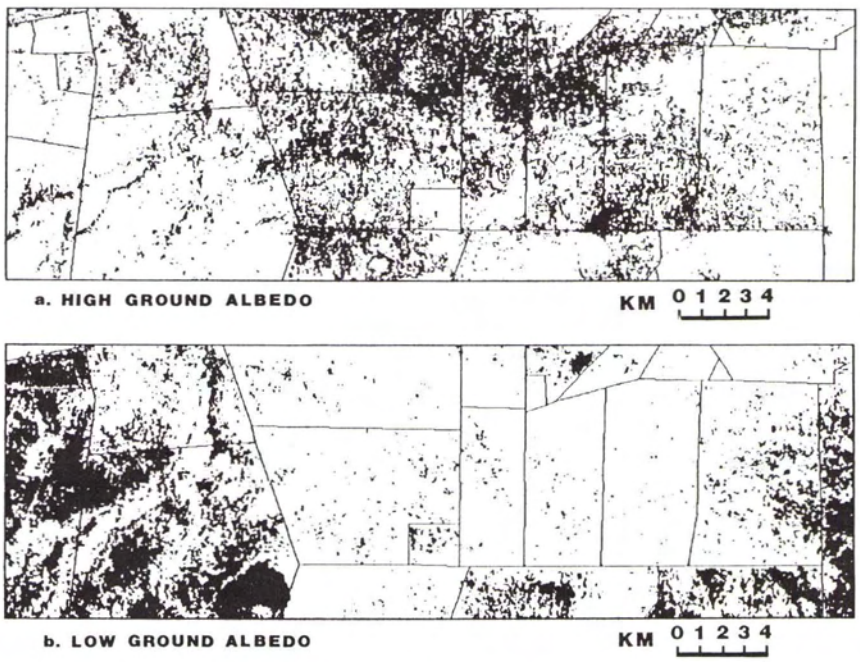

FIG. 10. (a) Intershrub ground albedo image, where all values greater than 0.35 are set to black. Based on ground truth sites, black zones correspond to those regions where a significant portion of the intershrub ground is gypsum or eroded soils. These regions are concentrated near wells (see Figure 3 (W)) or low evaporite areas (Figure 3 (G)). (b) Intershrub ground albedo image where all values less than 0.22 are black. Based on ground truth data, black areas correspond to those regions where a significant portion of the intershrub ground is covered by lichen, non-vigorous herbaceous plants or litter. Few dark regions are located within the central paddocks where lichen crust is generally absent. Within the OVR lichen forms a nearly continuous crust.

Within those areas where ground control was available, black areas can be shown to correspond to regions where gypsum or eroded soil make up a significant portion of the intershrub ground. The black regions of Figure 10a are mostly concentrated near wells where sheep grazing of herbaceous plants and the destruction of the soil lichen crust would be highest. The southeastern corners of a number of paddocks seem to be degraded also. This may reflect the movement of sheep into the prevailing wind (from the southeast; Crisp (1975)). A large expanse of high albedo ground is seen in the northern half of SLP and within the paddock to the north of it (Figure 3). This is a region that is periodically flooded after heavy rains. The subsequent evaporation of this water has concentrated gypsum in the soil so that locally it may reach 86 percent of the surface soil (Osborn *et al.*, 1932). Few degraded areas are located within the OVR, in agreement with the absence of scalds as observed by Crisp (1975).

Figure 10b shows areas that have calculated intershrub ground albedos less than 0.22 as black (an albedo of a shrubless model pixel with 50 percent lichen crust and 50 percent undisturbed soil). Within those areas where ground control was available, black regions can be shown to correspond to regions where lichen, non-vigorous herbaceous plants, or litter make up a significant portion of the intershrub ground cover. Note that those regions surrounding wells and within the paddocks toward the center of the study site show few regions of low calculated ground albedo (black). Crisp (1975) reports that the South Lake Paddock has almost no lichen crust. Figure 10b shows that low albedos are more abundant within the OVR (except in the south where high shrub cover prevents estimation of the intershrub ground albedo). This is consistent with near total cover by lichen crust within the OVR, as observed by Rogers (1974) and Crisp (1975). Field observations show that the re-established lichen crust between the woody perennial vegetation is one of the most noticeable differences between the OVR and adjacent areas (Sinclair, unpublished data, 1985).

The broad band of low albedos within the mapped *Eucalyptus* and *Acacia* association units, obvious in the albedo image (Figure 4), is not present in the intershrub ground albedo map (Figure 10b). Within these areas the low MSS albedo can be accounted for by high woody perennial vegetation cover, as revealed by high radar return in the SIR-A data. The elimination of the effect of woody perennial vegetation, whose spatial distribution crosses fence boundaries in Figure 4, reveals a pattern in the low ground albedo map (Figure 10b) where regions of low albedo are clearly correlated with fence boundaries, abundant in certain paddocks, and nearly absent in others. The low ground albedo map portrays the reflectance of a vegetation component (soil lichen and herbaceous vegetation), the condition of which is closely tied to the grazing of sheep and, thus, of utility to the range manager.

SUMMARY

Shrublands cover much of the interior of the Australiam continent and support a large grazing industry. Herbaceous plants are the preferred fodder of sheep, but during times of drought sheep graze almost exclusively on shrubs. Within semiarid shrublands both these vegetation components must be conserved to prevent significant resource degradation. Distinguishing the woody perennial vegetation from the smaller herbaceous vegetation and soil-encrusting lichen found between the shrubs is critical for range management but is difficult using Landsat data alone. In this study Shuttle Imaging Radar-A (SIR-A) and Landsat data are examined together over Koonamore Station. Given the low topography and fine textured soils such as those found at Koonamore, radar returns should be primarily determined by the percent area occupied by the woody vegetation component. During a period when most of the vegetation was non-vigorous and spectrally homogenous, SIR-A data, as a surrogate measure of shrub cover, allowed the reflectance due to shrubs in Landsat data to be separated to a first approximation from the reflectance due to the intervening ground. This method allows estimation of the intershrub reflectance properties that are related to herbaceous vegetation, lichen, and bare soil exposures. Calibrated radar backscatter data of the various species of woody vegetation present at Koonamore at various states of vigor would make these techniques more sensitive to intershrub signatures. Integration of radar image data into a range inventory can help distinguish areas of high herbaceous cover from those regions where woody perennial vegetation dominate even if both produce a similar response in images acquired in the reflected part of the visible/infrared spectrum.

ACKNOWLEDGMENTS

This work was supported by contracts to Washington University from the SIR-A Data Analysis Program (Jet Propulsion Laboratory Contact 956427) and the NASA Geology Program (JPL Contract 956515). Raymond E. Arvidson provided much valuable guidance and review during the entire long course of this work. Thanks go to Russ Sinclair, R. T. Lange, Stanley Morain, Charles J. Robinove, several anonomous reviewers, and to Ralph Kahn for critically reviewing the manuscript. Special thanks go to Mickey Eddy, Craig Leff, Pat Castillo, and to my office mates.

REFERENCES

Blom, R. G., and M. Daily, 1982. Radar image processing for rock-type discrimination, *IEEE Trans. on Geoscience and Remote Sensing*, v. GE-20, pp, 343–351.

Blom, R., and C. Elachi, 1981. Spaceborne and airborne imaging radar observations of sand dunes, *JGR*, v. 86, pp. 3061–3073.

Carrodus, B. B., R. L. Specht, and M. E. Jackman, 1965.

The vegetation of Koonamore Station, South Australia, *Trans. R. Soc. S. Aust.*, v. 89, pp. 41–59.

Courel, M.F., and M. Habif, 1983. Measurement of changes in Sahelian surface cover using Landsat albedo images, *Adv. Space Res.*, v. 2, pp. 37–44.

Crisp, M. D., 1975. *Long term change in arid zone vegetation at Koonamore, South Australia*, Ph.D. Thesis, Univ. of Adelaide.

———, 1978. Demography and survival under grazing of three Australian semi-desert shrubs, *Oikos*, v. 30, pp. 520–528.

Daily, M. I., T. Farr, C. Elachi, and G. Schaber, 1979. Geologic interpretation from composited radar and landsat imagery, *Photogram. Eng. and Remote Sensing*, v. 45, pp. 1109–1116.

Elachi, C., et al., 1982. Shuttle imaging radar experiment, *Science*, v. 218, pp. 996–1003.

Frank, T. D., 1984. The effect of change in vegetation cover and erosion patterns on albedo and texture of Landsat images in a semi-arid environment, *Ann. of Ass. of Am. Geographers*, v. 74, pp. 393–407.

Graetz, R. D., and M. R. Gentle, 1982. The relationship between reflectance in the landsat wavebands and the composition of an Australian semi-arid shrub rangeland, *Photogram. Eng. and Remote Sensing*, v. 48, pp. 1721–1730.

Graetz, R. D., M. R. Gentle, and R. P. Pech, 1982. The development and application of a landsat image-based resource information system (LIBRIS) and its application to the assessment and monitoring of Australian arid rangelands, *Proceedings of the International Symp. on Remote Sensing of Environ., First Thematic Conf., Remote Sensing of Arid Lands*, pp. 257–275.

Hall, E. A. A., R. L. Specht, and C. M. Eardley, 1964. Regeneration of the vegetation on Koonamore Vegetation Reserve, 1926–1962, *Aust. J. Bot.*, v. 12, pp. 205–264.

Henninger, D. L., and J. H. Carney, 1983. Shuttle Imaging Radar-A (SIR-A) data as a complement to Landsat Multispectral Scanner (MSS) data, *IGARSS*, FP-5, pp. 7.1–7.6.

Honey, F. R., and I. J. Tapley, 1982. Evaluation of shuttle SIR-A imagery for geologic and geomorphic mapping in N.W. Western Australia. *Proceedings of the International Symp. on Remote Sensing of Environ., Second Thematic Conf., Remote Sensing for Exploration Geology*, pp. 873–884.

Howard, J. A., 1977. Aerial albedos of natural vegetation in south-eastern Australia, *Proceedings of the 11th Symp. on Remote Sensing of Environ.*, pp. 1301–1307.

Kornblau, M. L., and J. E. Cipra, 1983. Investigation of digital landsat data for mapping soils under range vegetation, *Remote Sensing of Environ.*, v. 13, pp. 103–112.

Lane, I. R., 1982. Estimation of the forage production of semi-arid rangelands with variable tree and shrub cover using land resources satellites, *Proceedings of the International Symp. on Remote Sensing of Environ., First Thematic Conf., Remote Sensing of Arid Lands*, pp. 1169–1175.

Moore, R. M., 1973. Australian arid shrublands, *Arid Shrublands - Proceedings of the third workshop of the United States/Australia rangelands panel, Tucson:* Denver, Society for Range Management, pp. 6–11.

Morain, S. A., and J. B. Campbell, 1974. Reconnaissance soil surveys using radar imagery, *Proceedings Soil Science Society of America*, v. 38, pp. 818–826.

Morain, S. A., and D. S. Simonett, 1966. Vegetation analysis with radar imagery, *Proceedings of the Fourth International Symp. on Remote Sens. of Environ.*: University of Michigan, Ann Arbor, pp. 605–622.

Munday, T. J., 1982. Estimating the relative percentage of mineral salts in saline deposits of southern Tunisia using remotely sensed data, *Proceedings of the International Symp. on Remote Sensing of Environ., 2nd Thematic Conf., Remote Sensing for Exploration Geology*, pp. 903–914.

Musick, B. H., 1984. Assessment of Landsat multispectral scanner spectral indexes for monitoring arid rangeland, *IEEE Trans. on Geoscience and Remote Sensing*, v. GE-22, pp. 512–519.

Noble, I. R., 1977. Long-term biomass dynamics in an arid Chenopod shrub community at Koonamore, South Australia, *Aust. J. Bot.*, v. 25, pp. 639–653.

Osborn, T. G. B., J. G. Wood, and T. B. Paltridge, 1931. On the autecology of *Stipa nitida*, a study of a fodder grass in arid Australia, *Proc. Linn. Soc. N.S.W.*, v. 56, pp. 299–324.

———, 1932. On the growth and reaction to grazing of the perennial saltbush, *Atiplex vesicarium, Proc. Linn. Soc. N.S.W.*, v. 57, pp. 377–402.

———, 1935. On the climate and vegetation of the Koonamore Vegetation Reserve to 1931, *Proc. Linn. Soc. N.S.W.*, v. 1, pp. 392–427.

Otterman, J., and C. J. Robinove, 1981. Effects of the atmosphere on the detection of surface changes from Landsat multispectral scanner data, *Int. J. of Remote Sensing*, v. 2, pp. 351–360.

1983. Landsat monitoring of desert vegetation growth, 1972–1979 using a plant-shadowing mode, *Adv. Space Res.*, v. 8, pp. 45–50.

Richardson, A. J., 1981. Relating landsat digital count values to ground reflectance for optically thin atmospheric conditions, *Applied Optics*, v. 21, pp. 1457–1464.

Robinove, C. J., 1982. Computation with physical values from landsat digital data. *Photogram. Eng. and Remote Sensing*, v. 48, pp. 781–784.

Robinove, C. J., P. S. Gehring Jr., D. Gehring, and R. Holmgren, 1981. Arid land monitoring using Landsat albedo difference images, *Remote Sensing of Environ.*, v. 11, pp. 133–156.

Rogers, R. W., 1974. Lichens from the T. G. B. Osborn Vegetation Reserve at Koonamore in arid South Australia, *Trans. R. Soc. S. Aust.*, v. 98, pp. 113–124.

Rogers, R. W., and R. T. Lange, 1971. Lichen population on arid soil crusts around sheep watering places in South Australia, *Oikos*, v. 22, pp. 93–100.

Silander, Jr., J. A., 1983. Demographic variation in the Australian desert *cassia* under grazing pressure, *Oecologia*, v. 60, pp. 227–233.

Slatyer, R. O., 1973. Structure and function of Australian arid shrublands, *Arid Shrublands - Proceedings of the third workshop of the United States / Australia rangelands panel, Tucson*: Denver, Society for Range Management, pp. 66–73.

Tueller, P. T., F. R. Honey, and I. J. Tapley, 1978. Landsat and photographic remote sensing for arid land appli-

cations in Australia, *Proceedings 12th International Symp. on Remote Sensing of Environ.*, pp. 2177–2191.

Ulaby, F. T., 1981. Microwave response of vegetation, *Adv. Space Res.*, v. 1, pp. 55–70.

Walter, H., 1979. *Vegetation of the Earth and Ecological Systems of the Geo-Biosphere, Springer-Verlag, New York, pp. 91–103.*

Wood, J. G., 1936. Regeneration of the vegetation on the Koonamore Vegetation Reserve, 1926 to 1936. Trans. R. Soc. S. Aust., v. 60, pp. 96–111.

(Received 21 June 1985; accepted 30 September 1985; revised 14 January 1986)